Polygonum Barbatum Extract Reduces Colorectal Cancer Cell Proliferation, Migration, Invasion, and Epithelial-mesenchymal Transition via Regulation of the YAP and β-catenin Pathways

Pi-Kai Chang
National Defense Medical Center
I-Chuan Yen
National Defense Medical Center
Wei-Cheng Tsai
National Defense Medical Center
Shih-Yu Lee (leeshihyuno1@mail.ndmctsgh.edu.tw)
National Defense Medical Center https://orcid.org/0000-0002-4713-6410

Research

Keywords: colorectal cancer, Polygonum barbatum, epithelial-to-mesenchymal transition, YAP, GSK3β/β-catenin

Posted Date: October 12th, 2021

DOI: https://doi.org/10.21203/rs.3.rs-927177/v1

Abstract

Background

Colorectal cancer (CRC) is the third most common cancer worldwide, but the development of novel therapeutics for CRC remains a challenge. *Polygonum barbatum* has anticancer potential, but its mechanism of action requires further investigation. This study was designed to investigate the inhibitory effect of *Polygonum barbatum* on human CRC cells. The HPLC fingerprints of the *Polygonum barbatum* extract (PBE) and quercetin standard were determined using analytical RP-HPLC and evaluations were completed using the human colon cancer cell line HCT-116 (KRASG13D mutation) and HT-29 cells. After treatment with PBE, cell viability, colony formation, migration, invasion, and apoptosis were analyzed using CCK-8, colony formation, wound healing, Transwell invasion, and flow cytometry assays, respectively. RNA-sequencing, western blotting, and co-immunoprecipitation were also used to analyze changes in the whole-transcriptome of these cells and identify possible mechanisms of action for PBE in CRC cells.

Results

PBE significantly reduced CRC cell growth, migration, and invasion, and Gene Ontology analysis showed that the genes responsible for extracellular matrix organization, cell motility, and cell growth were suppressed by PBE. Kyoto Encyclopedia of Genes and Genomes pathway enrichment analysis of the differentially expressed genes revealed that PBE treatment exerted a significant effect on the extracellular matrix interaction and focal adhesion pathways. Consistently, epithelial-to-mesenchymal transition markers, including N-cadherin, vimentin, SLUG, and SNAIL, were also all shown to be regulated by PBE. These effects were associated with blockade of the Yes-associated protein and the GSK3β/β-catenin axis.

Conclusion

Polygonum barbatum extract exerts a significant inhibitory effect on CRC cells and may be potentially applicable in clinical trials.

Background

Colorectal cancer (CRC) is the third most commonly diagnosed cancer in the world, and both its incidence and mortality rates are increasing in Asia [1]. Treatments for unresectable metastatic CRC are designed to facilitate tumor shrinkage and control metastatic lesions, and a combination of targeted therapy and cytotoxic chemotherapies is commonly applied as the primary treatment for metastatic CRC. These treatments have resulted in a significant improvement in the median overall survival, from 12 to 30 months, over the last two decades [2]. Most patients experience some initial response to treatment, but many experience some degree of drug resistance over time, reducing efficacy. In addition, the high degree

of toxicity associated with the chemotherapy options for CRC also limit their long term application. This means that there is still an urgent need to develop novel therapeutic agents for CRC.

The Hippo pathway, including core kinase complexes MST1/2 and LATS1/2 and downstream effectors Yes-associated protein (YAP) and transcriptional coactivator with PDZ-binding motif (TAZ), regulates cell growth and differentiation acting as a tumor suppressor pathway [3]. Once activated, the Hippo pathway suppresses the nuclear translocation of YAP, which acts as an oncogene in most settings. The Hippo pathway is downregulated in a variety of cancer cells where YAP is known to be activate. YAP promotes the expression of various target genes, including connective tissue growth factor (CTGF) and cysteine-rich angiogenic inducer 61 (CYR61), which are associated with mesenchymal differentiation [4] and poor prognosis in CRC patients [5]. In addition, the Wnt signaling pathway regulates cell growth, epithelial-mesenchymal transition (EMT), and self-renewal, and aberrant WNT signaling has been associated with progression in CRC tissues [6, 7]. This makes these pathways ideal targets for new CRC therapies.

Polygonum barbatum, a perennial herb belonging to *the Polygonaceae* family, is widely distributed across Southeast Asia and generally grows in marshy ground near riversides and other aquatic environments [8]. *Polygonum barbatum* is known to possess antimicrobial activity [9] and its bioactive compounds have demonstrated anti-proliferative activity against non-small cell lung carcinoma (NCI-H640), breast cancer (MCF-7), and cervical cancer (HeLa) cells [10]. However, the effect of *Polygonum barbatum* treatment on CRC cells has not been described, and mechanistic insights into its action remain scarce. This study was designed to clarify the effects and underlying mechanism of *Polygonum barbatum* extracts (PBE) on CRC cells.

Methods

Instrumentation and analytical conditions

HPLC analysis of PBE and quercetin was performed on a Hitachi L-7100 instrument with a UV detector (L-2400), pump (L-2130), and autosampler (L-2200). Reverse-phase separation of the marker compound was performed using a Lichro CART® RP-18e (4.0 × 250 mm i.d., 5 μm) column and a gradient elution was achieved using two solvents, namely water (A) and methanol (B), at a flow rate of 1 mL/min. The gradient program consisted of an initial linear increase from 30% B to 60% B over 15 min, followed by an increase to 80% B over 15 min. This was then maintained for 10 min, and then returned to the initial gradient condition over the next 10 min before being maintained for another 5 min. The injection volume was 10 μL and the UV absorption spectra were recorded online at 370 nm, then the data were processed using the Hitachi Model D-2000 Elite Chromatography Data Station Software.

Cell culture and viability assays

Human colon cancer cell lines HCT-116 ($KRAS^{G13D}$ mutation) and HT-29 were obtained from the American Type Culture Collection (ATCC, Manassas, VA, USA) and cultured in DMEM with 10% fetal bovine serum

(FBS) at 37 °C. Cell viability was assayed using a Cell Counting kit-8 according to the manufacturer's instructions (CCK-8, Dojindo, Japan) [11].

Colony formation assay

This assay was completed as previously described [12]. Briefly, cells were incubated for 21 days at 37 °C using 0.5% agar in DMEM containing 10% FBS, 1 mM glutamine, 100 units penicillin, and 100 µg/mL streptomycin before the colonies were counted and quantified using ImageJ software version 1.50a (National Institutes of Health, Bethesda, MD, USA).

Migration and invasion assays

These assays were performed using Transwell cell culture chambers (8-µm), as previously described [13]. The Transwell inserts were coated with Matrigel (BD Biosciences, Bedford, MA, USA) prior to the invasion assay, but not the migration assay, and cells were seeded in the upper chamber and incubated in serum-free RPMI-1640 medium while the lower chamber was filled with medium supplemented with 10% FBS. Cells were added to the upper chamber and incubated for 24 h before being fixed in methanol and stained with crystal violet for 15 min. Cells at the bottom of the inserts were then counted using an inverted microscope.

Scratch assay

These assays were completed as previously described [14]. Briefly, HCT-116 and HT-29 cells were scratched using a 100 µL pipette tip, then washed with PBS and incubated with vehicle or PBE. Wound healing was imaged using photomicrography at various time points (Leica Microsystems, Wetzlar, Germany).

Flow cytometry

Cellular apoptosis was analyzed using an Annexin-V/7-AAD staining kit according to the manufacturer's instructions (BioVision, Inc., CA, USA). Cells were treated with vehicle or PBE and then stained with Annexin-V/7-AAD solution and analyzed using a flow cytometer (BD Biosciences, FACS CaliburTM) [12].

Nuclear extracts and western blotting

These assays were completed as previously described [15]. The details for the primary and secondary antibodies used in these assays are summarized in Table 1. The blots were developed using an enhanced chemiluminescence kit (Amersham Biosciences, Buckinghamshire, UK) and measured using a luminescent image analyzer (LAS-3000; Fuji Photo Film Co., Ltd., Tokyo, Japan).

Table 1. Antibodies used for Western blotting

Type	Antigen	Manufacturer	Dilution
Primary antibody	ZO-1	Proteintech	1:4000
Primary antibody	E-cadherin	GeneTex	1:2000
Primary antibody	N-cadherin	iReal Biotechnology	1:2000
Primary antibody	Fibronectin	Cell signaling	1:1000
Primary antibody	Vimentin	Abcam	1:1000
Primary antibody	Slug	Cell signaling	1:500
Primary antibody	Snail	GeneTex	1:500
Primary antibody	β-actin	Cell signaling	1:5000
Primary antibody	p-YAP 127	Applied Biological Materials Inc. (abm)	1:1000
Primary antibody	YAP	Cell signaling	1:1000
Primary antibody	TBP	arigo Biolaboratories	1:1000
Primary antibody	p-LATS1	Cell signaling	1:1000
Primary antibody	LATS1	Cell signaling	1:1000
Primary antibody	TAZ	Cell signaling	1:1000
Primary antibody	p-PTEN	Cell signaling	1:1000
Primary antibody	PTEN	Fine Test	1:1000
Primary antibody	p-AKT	Cell signaling	1:1000
Primary antibody	AKT	Cell signaling	1:1000
Secondary antibody	Anti-rabbit IgG-HRP	GeneTex	1:10000
Secondary antibody	Anti-mouse IgG-HRP	Jackson	1:10000

RNA sequencing

An RNA sequencing library was prepared using the TruSeq Stranded mRNA Library Prep Kit (Illumina, San Diego, CA, USA) and sequenced on an Illumina NovaSeq 6000 platform (150 bp paired-end reads) run by the Genomics, BioSci & Tech Co., New Taipei City, Taiwan. The quality of the libraries was assessed using an Agilent Bioanalyzer 2100 system and real-time PCR. The reads were mapped to the reference genome using Bowtie2 (version 2.3.4.1) [16]. Transcript abundance was quantified using RSEM (version 1.2.28) [17] and differentially expressed genes (DEGs) were identified using EBSeq (version 1.16.0) [18]. Gene Ontology (GO) and Kyoto Encyclopedia of Genes and Genomes (KEGG) pathway analysis were used to evaluate the gene clusters identified by the clusterProfiler program in R (version 3.6.0) [19].

Co-immunoprecipitation assays

These assays were performed as previously described [20]. Briefly, cells were lysed and incubated with anti-YAP beads for 4 h at 4°C, then washed before the immunocomplexes were suspended in SDS sample buffer and subjected to western blotting. The inputs were loaded with total cell lysates for comparison.

Statistical Analysis

All data are presented as the mean ± standard error of the mean (SEM) and the differences between groups were evaluated using one-way analysis of variance (ANOVA) and a Bonferroni post-hoc test. Statistical analyses were performed using IBM SPSS Statistics version 22 (IBM® SPSS® Statistics 22) and significance was accepted when the p values were less than 0.05.

Results

HPLC analysis of PBE

The retention time of quercetin was 17.13 min (Fig. 1A) and we produced a clear HPLC fingerprint for PBE (Fig. 1B).

PBE significantly inhibits cell growth and induces apoptosis in CRC cells

Annexin V/7-AAD staining showed that PBE treatment significantly increased the number of apoptotic cells in both HCT116 and HT29 cells (Figs. 2A-2D). These results were further confirmed by both cell viability (Figs. 2E and 2F) and colony formation (Figs. 2G–2J) assays with both showing significant reductions in response to PBE treatment. 5-Fluorouracil (5-FU) was used as the positive control. Taken together these results clearly indicate that PBE significantly reduces cell growth and induces apoptosis in CRC cells.

Differentially expressed mRNAs regulated by PBE

RNA sequencing of PBE-treated HCT-116 cells was used to identify the potential mechanism of action for this compound in CRC. The quality and read data for this sequencing experiment are summarized in Table 2. We identified 167 and 330 DEGs in cells treated with 30 μg/mL PBE (117 downregulated and 50 upregulated) and 100 μg/mL PBE (278 downregulated and 52 upregulated), respectively (Fig. 3A). DEG scatterplots visualize the differences between the vehicle control and 30 μg/mL PBE (Figure 3B), 100 μg/mL PBE (Figure 3C), or 5-FU (Figure 3D), respectively.

Table 2. Quality and read statistics for the RNA sequencing data

Sample	Clean data size (bp)	Clean reads number	Q30 (%)	Total mapped reads (%)
Control	6,193,238,770	21,901,128	95.37%	77.36%
PBE 30	4,756,679,235	17,279,188	95.10%	75.01%
PBE 100	5,637,303,528	20,925,391	95.13%	73.17%
5-FU	5,799,469,908	20,315,972	95.19%	74.53%

KEGG Pathway and GO Enrichment Analysis

KEGG and GO analysis were then used to further clarify the regulatory signaling pathway involved in PBE mediated inhibition of CRC cell proliferation, and the top 10 KEGG pathways for the DEGs in each group are shown in Table 3-5. We found that extracellular matrix (ECM)-receptor interactions and focal adhesion (FA) were the most significantly enriched pathways in PBE-treated cells (Figure 4A and 4B) and that these pathways included thrombospondin 1 (THBS1), glycoprotein Ib platelet subunit beta (GP1BB), laminin subunit alpha 5 (LAMA5), AGRN, integrin subunit beta 8 (ITGB8), tenascin XB (TNXB), heparan sulfate proteoglycan 2 (HSPG2), Fraser extracellular matrix complex subunit 1 (FRAS1), integrin subunit alpha 2 (ITGA2), fibronectin 1 (FN1), laminin subunit beta 2 (LAMB2), collagen type IV alpha 5 (COL4A5), integrin subunit alpha V (ITGAV), and SHC adaptor protein 3 (SHC3). In addition, GO enrichment analysis of the DEGs from the PBE-treated groups displayed significant enrichment for cellular proliferation and extracellular matrix organization (Figure 4C and 4D). Whole blood vessel morphogenesis was shown to be significantly enriched in the 5-FU group (Figure 4E). When we evaluated the GO terms associated with molecular function we found that both integrin binding and extracellular binding were significantly enriched in the PBE-treated cells (Figure 4F and 4G), while RNA polymerase II core promoter proximal region sequence-specific DNA binding was enriched in the 5-FU-treated cells (Figure 4H). In addition, both endocytic vehicle lumen and extracellular cellular components from the cellular component category were significantly enriched in the PBE-treated cells (Figure 4I and 4J), while adheren junctions was the most significantly enriched term in the 5-FU-treated cells (Figure 4K).

Table 3. KEGG Pathway enrichment of the Top 10 DEGs in the 30 ug/mL PBE group as identified by RNA sequencing

KEGG ID	Description	GeneRatio	*p* value
hsa04512	ECM-receptor interaction	5/50	0.000200515
hsa05144	Malaria	4/50	0.000246013
hsa05143	African trypanosomiasis	3/50	0.001511117

Table 4. KEGG Pathway enrichment of the Top 10 DEGs in the 100 ug/mL PBE group as identified by RNA sequencing

KEGG ID	Description	GeneRatio	*p* value
hsa04512	ECM-receptor interaction	13/113	2.0363E-10
hsa04933	AGE-RAGE signaling pathway in diabetic complications	7/113	0.000487805
hsa04510	Focal adhesion	10/113	0.000500723
hsa05165	Human papillomavirus infection	13/113	0.000711372
hsa04151	PI3K-Akt signaling pathway	13/113	0.00132048
hsa05222	Small cell lung cancer	6/113	0.001794871
hsa04974	Protein digestion and absorption	6/113	0.002114667
hsa05031	Amphetamine addiction	5/113	0.002746707

Table 5. KEGG Pathway enrichment of the Top 10 DEGs in the 5-FU-treated group as identified by RNA sequencing

KEGG ID	Description	GeneRatio	*p* value
hsa04390	Hippo signaling pathway	21/188	7.11685E-11
hsa04510	Focal adhesion	20/188	3.85421E-08
hsa05205	Proteoglycans in cancer	20/188	5.37371E-08
hsa04010	MAPK signaling pathway	24/188	7.43009E-08
hsa05219	Bladder cancer	9/188	3.14295E-07
hsa05210	Colorectal cancer	12/188	6.28017E-07
hsa04115	p53 signaling pathway	10/188	6.59901E-06
hsa05225	Hepatocellular carcinoma	15/188	8.11604E-06
hsa04810	Regulation of actin cytoskeleton	17/188	9.65181E-06
hsa05224	Breast cancer	13/188	3.67231E-05

PBE significantly inhibits cell migration, invasion, and epithelial-to-mesenchymal transition (EMT) in CRC cells

Wound healing, cell migration, and invasion assays were used to elucidate the effects of PBE on CRC cells. We found that PBE significantly inhibited the wound healing rate in both HCT-116 (Figs. 5A and 5 B) and HT-29 (Figs. 5C and 5D) cells. Similar inhibitory effects were observed in the migration assays (Figure 5E and 5F) and we found that the invasion rates of PBE-treated cells were significantly lower than those of the vehicle control (Figure 5G and 5H). In addition, we went on to evaluate the EMT-associated markers using western blotting. We found that the levels of epithelial markers ZO-1 and E-cadherin were increased in PBE-treated cells when compared with the control in both HCT-116 (Figs 5I, 5J, and 5 K) and HT-29 cells (Figs 5P, 5Q, and 5R). In contrast, mesenchymal markers, including N-cadherin, fibronectin, vimentin, SLUG, and SNAIL all decreased in response to PBE treatment in both HCT-116 (Figs. 5I, 5 L, 5M, 5N, and 5O) and HT-29 cells (Figs. 5P, 5S, 5T, 5U, and 5V). These findings indicate that PBE inhibits migration, invasion, and EMT in CRC cells.

PBE blocks the YAP signaling pathway

We then used western blot to explore the molecular mechanisms underlying the effects of PBE in CRC cells. We found that PBE (100 μg/mL) significantly increased the S127 phosphorylation of YAP in both cell lines (Figs. 6A-6D). In addition, the levels of p-YAP increased in a dose-dependent manner following the addition of PBE (Figs. 6E-6G). This was then confirmed by evaluating both cytoplasmic and nuclear extracts in more detail. PBE treatment significantly reduced the nuclear translocation of YAP, but did not change the cytosolic retention of this protein (Figs. 6I-6N). Meanwhile, PBE treatment reduced the expression of YAP target genes CTGF and CYR61 (Figs. 6O-6R). These results reveal that PBE treatment significantly suppresses YAP signaling. In addition, co-immunoprecipitation revealed that the interaction between glycogen synthase kinase 3β (GSK3β), β-catenin, and YAP increased in PBE-treated cells (Fig. 6S). This implies that PBE also regulates the WNT signaling pathway.

PBE suppresses the GSK3β/β-catenin signaling pathway

We then went on to confirm the role of PBE in the regulation of WNT signaling by evaluating the GSK3β/β-catenin signaling pathway. As expected, PBE significantly reduced the phosphorylation of GSK3β at Ser9 in both a time (Figs. 7A-7D) and dose dependent manner (Figs. 7E-7H) in both cell lines. Consistently, the nuclear and cytosolic protein levels of β-catenin were also shown to be modulated by PBE treatment (Figs. 7I-7N). We further investigated the downstream targets of the Wnt pathway and demonstrated that PBE treatment significantly increased the phosphorylation of β-catenin and its targets, including cyclin D1, c-Myc, and c-Jun, which were downregulated in both cell lines (Figs. 7O-7X). These findings indicate that PBE inhibits the WNT/β-catenin signaling pathway in CRC cells.

Discussion

PBE significantly reduced motility and tumorigenic potential by modulating EMT in both HCT116 and HT29 CRC cells. PBE treatment triggered cellular apoptosis, as established by an annexin V-FITC and 7-AAD double stain assay. Both GO and KEGG analysis of the RNA sequencing data was consistent with these findings, with this analysis demonstrating that the expression of the genes responsible for extracellular matrix organization (CTGF and CYR61), cell motility (THBS1 and CXCL8), and cell growth (PLXNB1 and FN1) were all inhibited by PBE. These effects are associated with the blockage of both YAP and Wnt signaling (Fig. 8).

Polygonum barbatum has been reported to produce potential anticancer bioactive compounds such as dihydrobenzofuran, sesquiterpene derivatives [10, 21], and quercetin [22]. Quercetin has been shown to activate the Hippo pathway and inhibit YAP signaling [23], and sesquiterpene derivatives have been reported to induce ROS- and TRAIL-mediated apoptosis, enhance chemotherapy responses, and inhibit EMT with these effects being accompanied by the downregulation of β-catenin in CRC cells [24]. To the best of our knowledge, this is the first study to show that *Polygonum barbatum* can reduce the migration and tumorigenic potential of CRC cells by blocking both YAP and β-catenin signaling. Based on these findings, these bioactive compounds are thought to synergistically contribute to the anti-CRC properties of PBE. However, most of these findings are based on *in vitro* studies, which means that further *in vivo*

evaluations and clinical trials are required to make any definitive statements on their activity. Interestingly, 2,3-dihydrobenzofuran derivatives have been shown to exhibit microsomal prostaglandin E2 synthase-1 inhibitor activity [25], a key enzyme in prostaglandin E2 (PGE_2) synthesis known to boost CRC immune evasion [26]. Therefore, the regulatory effect of PBE on the COX-2/PGE_2 axis, and its mediators such as Janus kinase 2/signal transducer and activator of transcription 3 in CRC, will be investigated in our future work.

The ECM regulates cellular behavior and participates in both cellular adhesion and migration, with the overexpression of ITGAV, ITGA1, ITGB8, and FN genes known to be involved in CRC growth and metastasis [27-29][30]. In addition, collagen XII, FRAS1, LAMA5, and THBS1 are all associated with colorectal liver metastasis, which is the most common distant metastasis in CRC patients [31] [32] [33]. In this study, our GO and KEGG analyses of the RNA sequencing data revealed that both the ECM and FA pathways were significantly downregulated in response to PBE. When combined with the results from the apoptosis evaluations we can confirm that these outcomes are consistent with the finding that diminished expression of ITGA2 promotes death and apoptosis in CRC cells [34]. Interestingly, we found that GP1BB, a regulator of epithelial cell adhesion, was upregulated in response to PBE treatment. This regulator has been reported to increase cell-cell contact, leading to the downregulation of EMT [35]. Consistently, cell mobility, invasion, and EMT were also shown to be inhibited by PBE. These findings indicate that PBE is able to inhibit the ECM-receptor interaction and FA pathways, suppressing cell migration, invasion, and EMT. ECM and FA are also involved in the regulation of many signaling pathways, including the Hippo pathway. Low ECM resistance and FA correspond to reduced mechanics and subsequently regulate the Hippo pathway [36]. YAP/TAZ, the major effector of the Hippo pathway, senses alterations in ECM composition [37] and its downstream targets CYR61 and CTGF are upregulated. This upregulation has been linked to drug resistance and RAS/MAPK blockade in CRC cells, indicating their critical role in RAS-mutated metastasis and drug resistance [38] [39] [40] [41]. Here we found that PBE treatment blocked YAP signaling and its downstream gene expression. This indicates that PBE inhibits CRC progression by regulating YAP signaling, which is closely associated with EMT progression. PBE also inhibited several EMT markers, including SNAIL, TWIST, and SLUG. We also showed that PBE was able to inhibit cell growth, invasion, and migration in both HCT116 and HCT29 cells. Based on these findings we suggest that PBE might exhibit synergistic effects with 5-Fu and EGFR inhibitors (cetuximab) when used to treat CRC. However, this requires further investigation. YAP is regulated by the Hippo pathway, including MST1/2 and LATS1/2, which interacts with the phosphatase and tensin homolog /AKT/ mechanistic target of rapamycin autophagic axis [42]. However, the role of autophagy in CRC remains unclear and still requires further in-depth mechanistic studies to be fully understood [43]. Given this, it would be interesting to investigate the role of PBE in the modulation of autophagy and the regulation of YAP via the Hippo pathway.

Approximately 50% of patients with CRC present with mutations in the β-catenin gene [44]. This means that WNT/β-catenin signaling is a potential therapeutic target for CRC. We found that PBE treatment decreased the nuclear translocation of β-catenin by increasing β-catenin, GSK-3β, and YAP complex

formation, which blocked β-catenin-mediated oncogenic signaling and inhibited invasion, migration, and EMT progression. Hippo signaling also interacts with Notch signaling to suppress liver tumorigenesis [45] and LAMA5 expression is associated with Notch signaling, which promotes EMT by interacting with *SLUG* and *SNAIL* [33]. Based on the inhibitory effect of PBE on EMT, it would be interesting to investigate the regulatory role of PBE in Notch signaling, which has already been tightly linked to CRC progression [46]. However, this requires further investigation. In this study, we showed that PBE exerts a significant inhibitory effect on the two main signaling pathways (YAP and Wnt/β-catenin) associated with CRC progression. However, KRAS mutations and PI3K/AKT activation play important roles in drug resistance [47], and PBE exerts equal inhibitory effects in both KRAS mutant and wild-type CRC cells. It would be interesting to investigate the synergistic effect of PBE and EGFR inhibitors in the treatment of CRC in future work.

Conclusions

Our findings suggest that *Polygonum barbatum* exerts an inhibitory effect on CRC cell motility and tumorigenic potential, making these extracts a potential therapeutic for this type of cancer. We suggest that this makes it an appropriate candidate for future clinical trials.

Abbreviations

CRC: Colorectal cancer; PBE: *Polygonum barbatum* extract; YAP: Yes-associated protein; TAZ: transcriptional coactivator with PDZ-binding motif; CTGF: connective tissue growth factor; CYR61: cysteine-rich angiogenic inducer 61; EMT: epithelial-mesenchymal transition; ATCC: American Type Culture Collection; FBS: fetal bovine serum; CCK-8: Cell Counting kit-8; DEGs: differentially expressed genes; GO: Gene Ontology; KEGG: Kyoto Encyclopedia of Genes and Genomes; SEM: standard error of the mean; NGS: next-generation sequencing; ECM: extracellular matrix; FA: focal adhesion; THBS1: thrombospondin 1; GP1BB: glycoprotein Ib platelet subunit beta; LAMA5: laminin subunit alpha 5; ITGB8: integrin subunit beta 8; TNXB: tenascin XB; HSPG2: heparan sulfate proteoglycan 2; FRAS1: Fraser extracellular matrix complex subunit 1; ITGA2: integrin subunit alpha 2; FN1: fibronectin 1; LAMB2: laminin subunit beta 2; COL4A5: collagen type IV alpha 5; ITGAV: integrin subunit alpha V; SHC3; SHC adaptor protein 3; GSK3β: glycogen synthase kinase 3β; PGE_2: prostaglandin E2

Declarations

Acknowledgments

The authors thank the financial support from the Ministry of Science and Technology (MOST 108-2320-B-016-008-MY3 to S.-Y. L.) Taipei, Taiwan

Author Contributions: Conceptualization, Pi-Kai Chang and SHIH-YU LEE; Data curation, I-Chuan Yen and Wei-Cheng Tsai; Formal analysis, I-Chuan Yen and Wei-Cheng Tsai; Funding acquisition, SHIH-YU LEE;

Investigation, Pi-Kai Chang and Wei-Cheng Tsai; Methodology, I-Chuan Yen and Wei-Cheng Tsai; Project administration, Pi-Kai Chang, Wei-Cheng Tsai and SHIH-YU LEE; Resources, I-Chuan Yen and SHIH-YU LEE; Supervision, SHIH-YU LEE; Validation, I-Chuan Yen; Writing – original draft, Pi-Kai Chang; Writing – review & editing, SHIH-YU LEE.

Funding

The financial support from the Ministry of Science and Technology (MOST 108-2320-B-016-008-MY3 to S.-Y. L.) Taipei, Taiwan

Availability of data and materials

The datasets used and/or analysed during the current study are available from the corresponding author upon request.

Ethics approval and consent to participate

Not applicable.

Consent for publication

Not applicable.

Competing interests

The authors declare no conflict of interest

References

1. E.F. Onyoh, W.F. Hsu, L.C. Chang, Y.C. Lee, M.S. Wu, and H.M. Chiu. "The Rise of Colorectal Cancer in Asia: Epidemiology, Screening, and Management," Curr Gastroenterol Rep, vol. 21, no. 8, p. 36.

2. M.G. Fakih. "Metastatic colorectal cancer: current state and future directions," J Clin Oncol, vol. 33, no. 16, pp. 1809-1824.

3. Zhipeng Meng, Toshiro Moroishi, and K.-L. Guan. "Mechanisms of Hippo pathway regulation," Genes Dev, vol. 30, no. 1, pp. 1-17.

4. G.T.K. Boopathy and W. Hong. "Role of Hippo Pathway-YAP/TAZ Signaling in Angiogenesis," Front Cell Dev Biol, vol. 7, p. 49.

5. H.F. Yuen, C.M. McCrudden, Y.H. Huang, et al. "TAZ expression as a prognostic indicator in colorectal cancer," PLoS One, vol. 8, no. 1, p. e54211.

6. E.M. Schatoff, B.I. Leach, and L.E. Dow. "Wnt Signaling and Colorectal Cancer," Curr Colorectal Cancer Rep, vol. 13, no. 2, pp. 101-110.

7. T. Reya and H. Clevers. " Wnt signalling in stem cells and cancer.," Nature, vol. 434, no. 7035, pp. 843-850.

8. V. Kott, L. Barbini, M. Cruanes, et al. "Antiviral activity in Argentine medicinal plants," J Ethnopharmacol, vol. 64, no. 1, pp. 79-84.

9. S. Khan, U. Farooq, A. Khan, S. Naz, R. Sarwar, and N. Mirza. "Antimicrobial potential and physio-chemical analysis of Polygonum barbatum," L J Chem Soc Pak, vol. 36, no. 4, p. 687.

10. U. Farooq, S. Naz, B. Zehra, et al. "Isolation and characterization of three new anti-proliferative Sesquiterpenes from Polygonum barbatum and their mechanism via apoptotic pathway," BMC Cancer, vol. 17, no. 1, p. 694.

11. C.-H. Wu, C.-H. Ou, I.C. Yen, and S.-Y. Lee. "4-Acetylantroquinonol B Inhibits Osteoclastogenesis by Inhibiting the Autophagy Pathway in a Simulated Microgravity Model," Int J Mol Sci, vol. 21, no. 18, p. 6971.

12. Y.-L. Chen, I.C. Yen, K.-T. Lin, F.-Y. Lai, and S.-Y. Lee. "4-Acetylantrocamol LT3, a New Ubiquinone from Antrodia cinnamomea, Inhibits Hepatocellular Carcinoma HepG2 Cell Growth by Targeting YAP/TAZ, mTOR, and WNT/β-Catenin Signaling," The American Journal of Chinese Medicine, vol. 48, no. 05, pp. 1243-1261.

13. D. Jeong, S. Park, H. Kim, et al. "RhoA is associated with invasion and poor prognosis in colorectal cancer," Int J Oncol, vol. 48, no. 2, pp. 714-722.

14. S.Y. Lee, I.C. Yen, J.C. Lin, M.C. Chung, and W.H. Liu. "4-Acetylantrocamol LT3 Inhibits Glioblastoma Cell Growth and Downregulates DNA Repair Enzyme O(6)-Methylguanine-DNA Methyltransferase," Am J Chin Med, pp. 1-17.

15. L.Y. Huang, I.C. Yen, W.C. Tsai, and S.Y. Lee. "Rhodiola crenulata Suppresses High Glucose-Induced Matrix Metalloproteinase Expression and Inflammatory Responses by Inhibiting ROS-Related HMGB1-TLR4 Signaling in Endothelial Cells," Am J Chin Med, vol. 48, no. 1, pp. 91-105.

16. B. Langmead and S.L. Salzberg. "Fast gapped-read alignment with Bowtie 2," Nat Methods, vol. 9, no. 4, pp. 357-359.

17. B. Li and C.N. Dewey. "RSEM: accurate transcript quantification from RNA-Seq data with or without a reference genome," BMC Bioinformatics, vol. 12, p. 323.

18. N. Leng, J.A. Dawson, J.A. Thomson, et al. "EBSeq: an empirical Bayes hierarchical model for inference in RNA-seq experiments," Bioinformatics, vol. 29, no. 8, pp. 1035-1043.

19. G. Yu, L.G. Wang, Y. Han, and Q.Y. He. "clusterProfiler: an R package for comparing biological themes among gene clusters," OMICS, vol. 16, no. 5, pp. 284-287.

20. L. Azzolin, T. Panciera, S. Soligo, et al. "YAP/TAZ incorporation in the beta-catenin destruction complex orchestrates the Wnt response," Cell, vol. 158, no. 1, pp. 157-170.

21. U. Farooq, S. Naz, A. Shams, et al. "Isolation of dihydrobenzofuran derivatives from ethnomedicinal species Polygonum barbatum as anticancer compounds," Biological Research, vol. 52, no. 1.

22. T. Uttarawichien, C. Kamnerdnond, T. Inwisai, P. Suwannalert, N. Sibmooh, and W. Payuhakrit. "Quercetin Inhibits Colorectal Cancer Cells Induced-Angiogenesis in Both Colorectal Cancer Cell and Endothelial Cell through Downregulation of VEGF-A/VEGFR2," Scientia Pharmaceutica, vol. 89, no. 2, p. 23.

23. D. Lei, L. Chengcheng, Q. Xuan, et al. "Quercetin inhibited mesangial cell proliferation of early diabetic nephropathy through the Hippo pathway," Pharmacol Res, vol. 146, p. 104320.

24. T. Abu-Izneid, A. Rauf, M.A. Shariati, et al. "Sesquiterpenes and their derivatives-natural anticancer compounds: An update," Pharmacol Res, vol. 161, p. 105165.

25. S. Di Micco, C. Spatafora, N. Cardullo, et al. "2,3-Dihydrobenzofuran privileged structures as new bioinspired lead compounds for the design of mPGES-1 inhibitors," Bioorg Med Chem, vol. 24, no. 4, pp. 820-826.

26. D. Wang and R.N. Dubois. "Eicosanoids and cancer," Nat Rev Cancer, vol. 10, no. 3, pp. 181-193.

27. Jaques Waisberg, Luciano De Souza Viana, Renato José Affonso Junior, et al. "Overexpression of the ITGAV gene is associated with progression and spread of colorectal cancer," Anticancer Res, vol. 34, no. 10, pp. 5599-5607.

28. H. Li, Y. Wang, S.K. Rong, et al. "Integrin alpha1 promotes tumorigenicity and progressive capacity of colorectal cancer," Int J Biol Sci, vol. 16, no. 5, pp. 815-826.

29. Liang Huang, Jin Lin Cai, Pin Zhu Huang, et al. "miR19b-3p promotes the growth and metastasis of colorectal cancer via directly targeting ITGB8," Am J Cancer Res, vol. 7, no. 10, pp. 1996-2008.

30. Xun Cai, Chuan Liu, Tie-Ning Zhang, Yi-Wen Zhu, Xiao Dong, and P. Xue. "Down-regulation of FN1 inhibits colorectal carcinogenesis by suppressing proliferation, migration, and invasion," J Cell Biochem, vol. 119, no. 6, pp. 4717-4728.

31. N.A. van Huizen, R.R.J. Coebergh van den Braak, M. Doukas, L.J.M. Dekker, I.J. JNM, and T.M. Luider. "Up-regulation of collagen proteins in colorectal liver metastasis compared with normal liver tissue," J Biol Chem, vol. 294, no. 1, pp. 281-289.

32. Q. Zhi, D. Wan, R. Ren, et al. "Circular RNA profiling identifies circ102049 as a key regulator of colorectal liver metastasis," Mol Oncol, vol. 15, no. 2, pp. 623-641.

33. A. Gordon-Weeks, S.Y. Lim, A. Yuzhalin, et al. "Tumour-Derived Laminin alpha5 (LAMA5) Promotes Colorectal Liver Metastasis Growth, Branching Angiogenesis and Notch Pathway Inhibition," Cancers (Basel), vol. 11, no. 5.

34. Y. Xu, L. Shen, F. Li, J. Yang, X. Wan, and M. Ouyang. "microRNA-16-5p-containing exosomes derived from bone marrow-derived mesenchymal stem cells inhibit proliferation, migration, and invasion, while promoting apoptosis of colorectal cancer cells by downregulating ITGA2," J Cell Physiol, vol. 234, no. 11, pp. 21380-21394.

35. R.A. Al-Temaimi, T.Z. Tan, M.J. Marafie, J.P. Thiery, P. Quirke, and F. Al-Mulla. "Identification of 42 Genes Linked to Stage II Colorectal Cancer Metastatic Relapse," Int J Mol Sci, vol. 17, no. 5.

36. A. Totaro, T. Panciera, and S. Piccolo. "YAP/TAZ upstream signals and downstream responses," Nat Cell Biol, vol. 20, no. 8, pp. 888-899.

37. G. Nardone, J. Oliver-De La Cruz, J. Vrbsky, et al. "YAP regulates cell mechanics by controlling focal adhesion assembly," Nat Commun, vol. 8, p. 15321.

38. R. Ladwa, H. Pringle, R. Kumar, and K. West. "Expression of CTGF and Cyr61 in colorectal cancer," J Clin Pathol, vol. 64, no. 1, pp. 58-64.

39. Lijuan Wang, Shengjia Shi, Zhangyan Guo, et al. "Overexpression of YAP and TAZ Is an Independent Predictor of Prognosis in Colorectal Cancer and Related to the Proliferation and Metastasis of Colon Cancer Cells," PLoS One, vol. 8, no. 6, p. e65539.

40. K. Yang, K. Gao, G. Hu, Y. Wen, C. Lin, and X. Li. "CTGF enhances resistance to 5-FU-mediating cell apoptosis through FAK/MEK/ERK signal pathway in colorectal cancer," Onco Targets Ther, vol. 9, pp. 7285-7295.

41. B.S. Liu, H.W. Xia, S. Zhou, et al. "Inhibition of YAP reverses primary resistance to EGFR inhibitors in colorectal cancer cells," Oncol Rep, vol. 40, no. 4, pp. 2171-2182.

42. W. Xu, M. Zhang, Y. Li, et al. "YAP manipulates proliferation via PTEN/AKT/mTOR-mediated autophagy in lung adenocarcinomas," Cancer Cell Int, vol. 21, no. 1, p. 30.

43. S.N. Devenport and Y.M. Shah. "Functions and Implications of Autophagy in Colon Cancer," Cells, vol. 8, no. 11.

44. X. Cheng, X. Xu, D. Chen, F. Zhao, and W. Wang. "Therapeutic potential of targeting the Wnt/beta-catenin signaling pathway in colorectal cancer," Biomed Pharmacother, vol. 110, pp. 473-481.

45. W. Kim, S.K. Khan, J. Gvozdenovic-Jeremic, et al. "Hippo signaling interactions with Wnt/beta-catenin and Notch signaling repress liver tumorigenesis," J Clin Invest, vol. 127, no. 1, pp. 137-152.

46. A. Tyagi, A.K. Sharma, and C. Damodaran. "A Review on Notch Signaling and Colorectal Cancer," Cells, vol. 9, no. 6.

47. T. Vu and P.K. Datta. "Regulation of EMT in Colorectal Cancer: A Culprit in Metastasis," Cancers (Basel), vol. 9, no. 12.

Figures

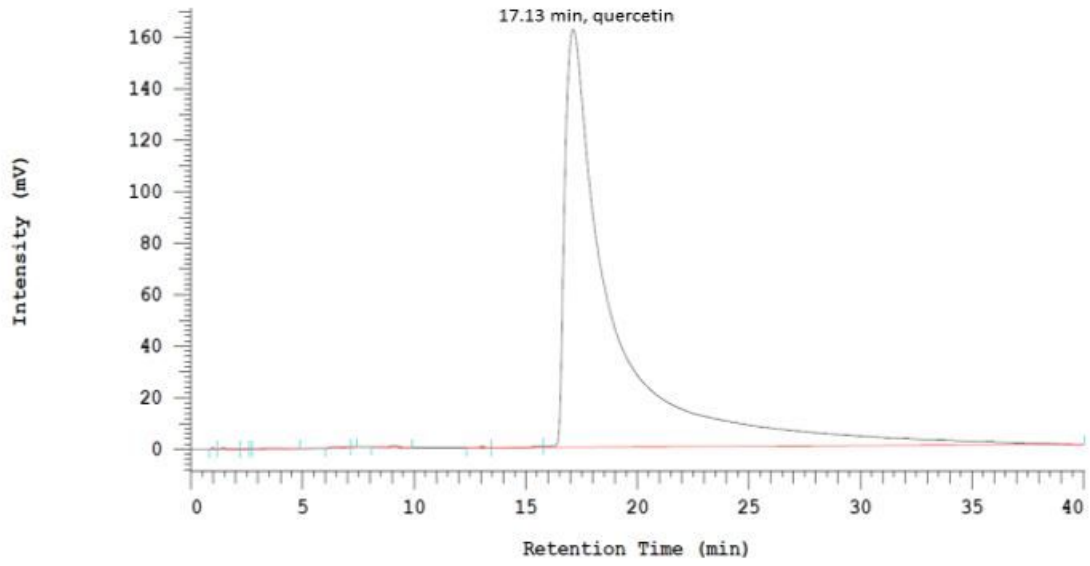

(A)

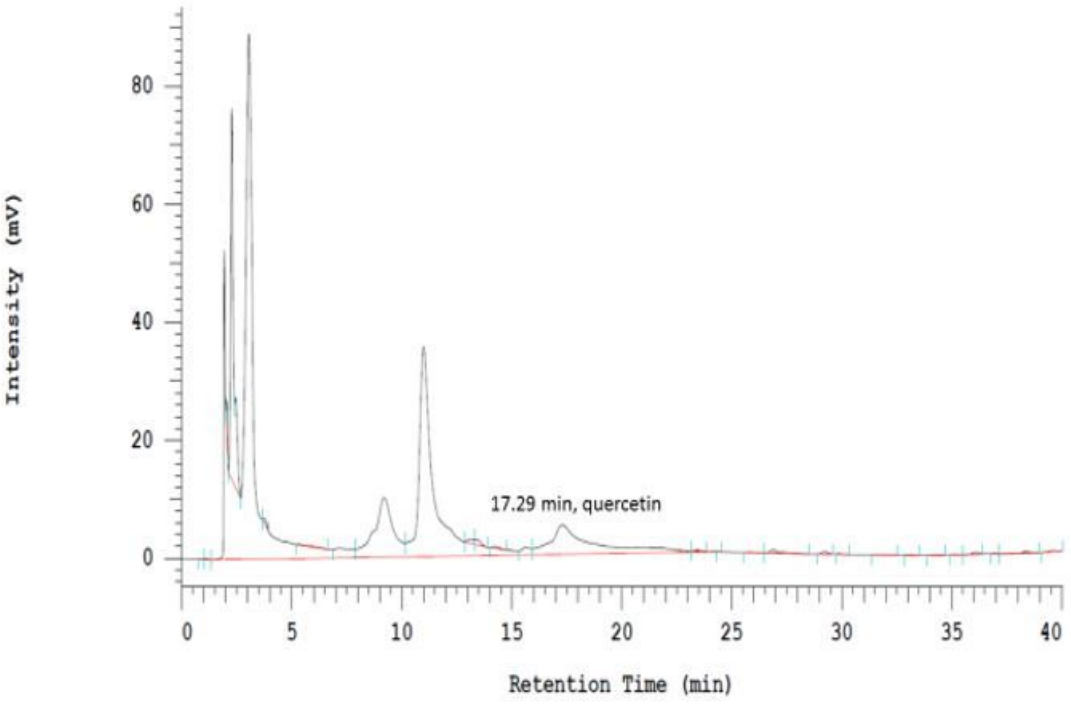

(B)

Figure 1

HPLC fingerprint of the Polygonum barbatum extract (PBE) (A) and quercetin (B). The amount of the active marker (quercetin) was determined using analytical RP-HPLC and a methanol–water gradient. The peaks were detected by UV light, and the analytes were quantified at 370 nm.

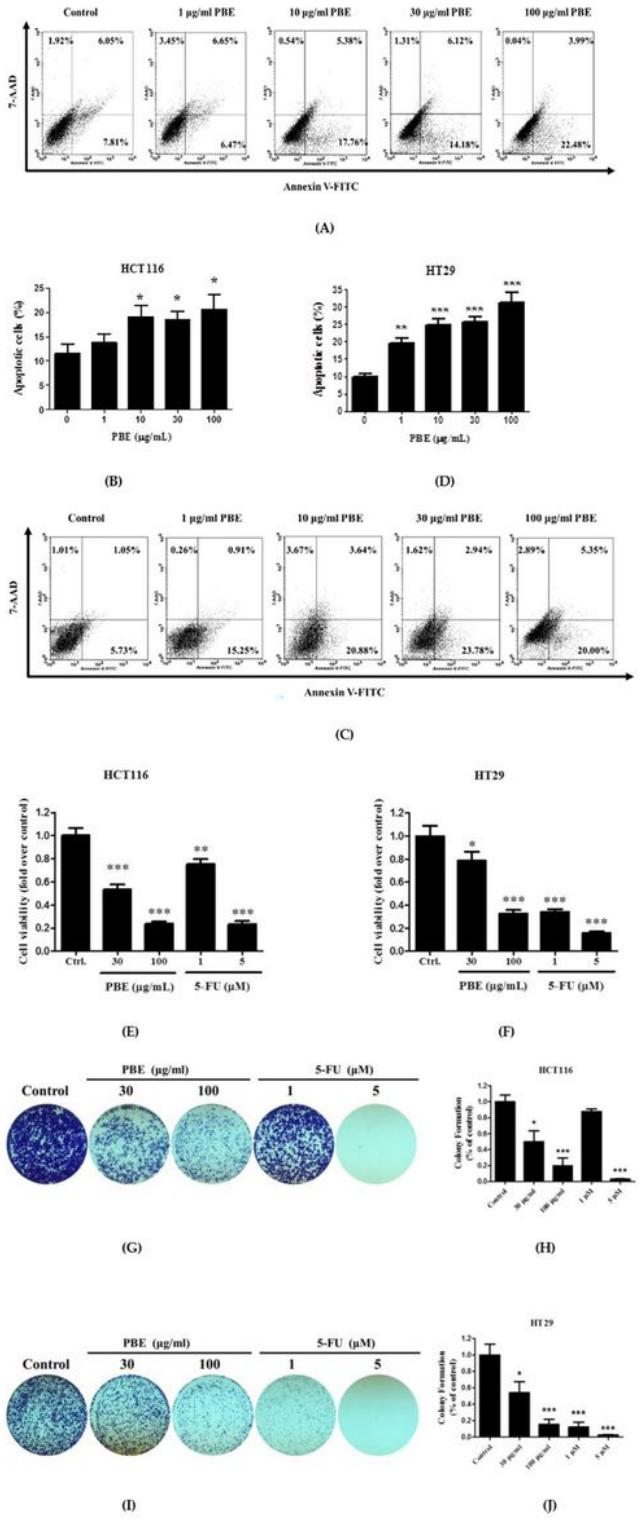

Figure 2

Effects of PBE treatment on apoptosis and viability in CRC cell lines. HCT116 and HT29 cells were treated with different concentrations (1-100 μg/mL) of PBE and then evaluated for apoptosis using annexin V/7-AAD double staining at 72 h (A and C). Percentage of annexin V-positive cells (B and D). Cell viability was measured using a CCK-8 kit following 72 h of PBE exposure (E and F) and colony formation was visualized using crystal violet staining following 14 days of PBE treatment (G and I). Quantitative

analysis of the colony formation assay (H and J). 5-FU was used as a positive control. Data are presented as the mean ± SEM from three independent experiments. *p<0.05, **p<0.01, and ***p<0.001 vs vehicle-treated cells.

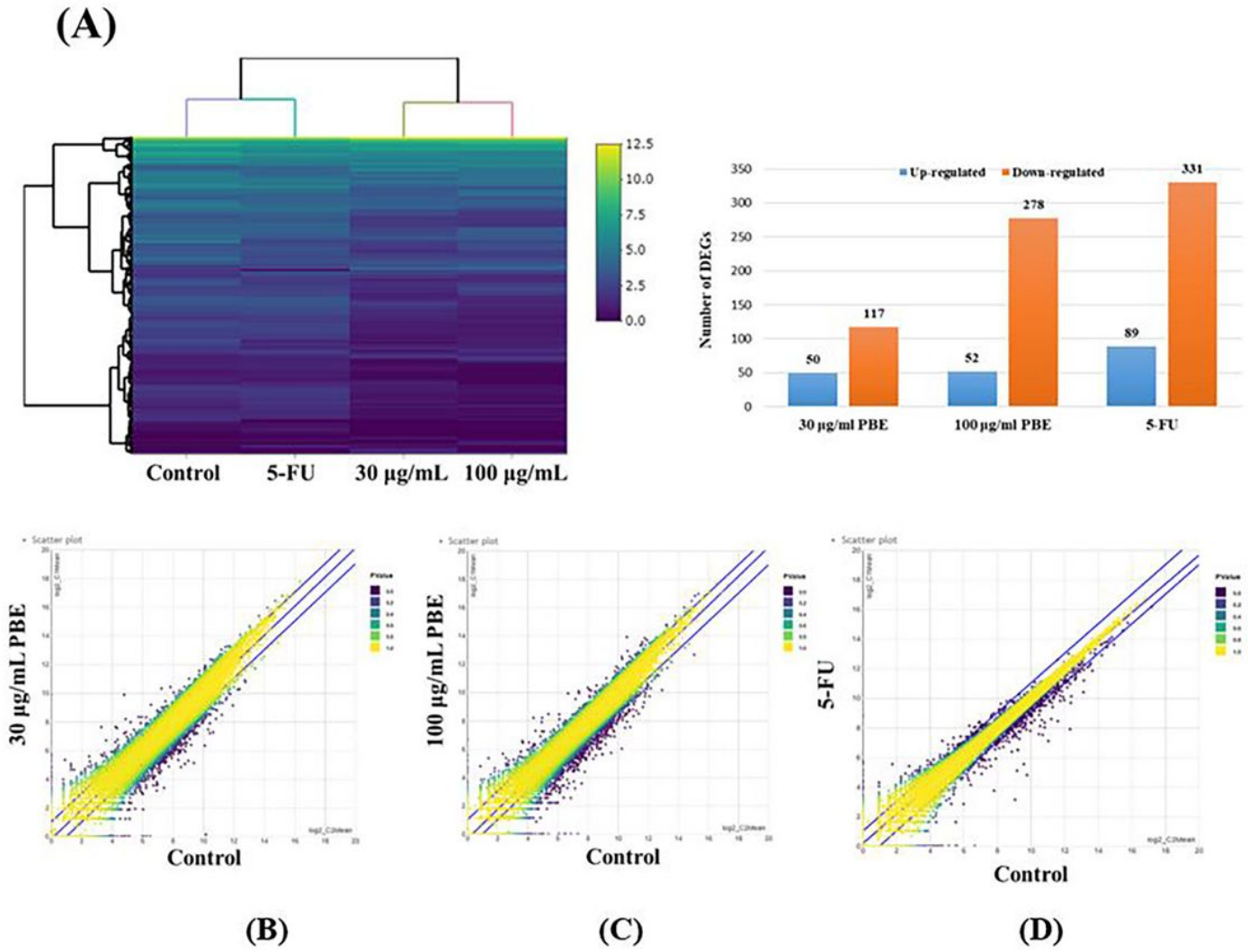

Figure 3

Transcriptomic profiles of PBE-treated HCT116 cells were determined using next-generation sequencing (NGS). HCT116 cells were treated with vehicle, PBE (30 and 100 μg/mL), or 5-FU (1 μM) and then subjected to RNA sequencing. DEGs (A) and DEG scatterplots (B, C, and D) are shown.

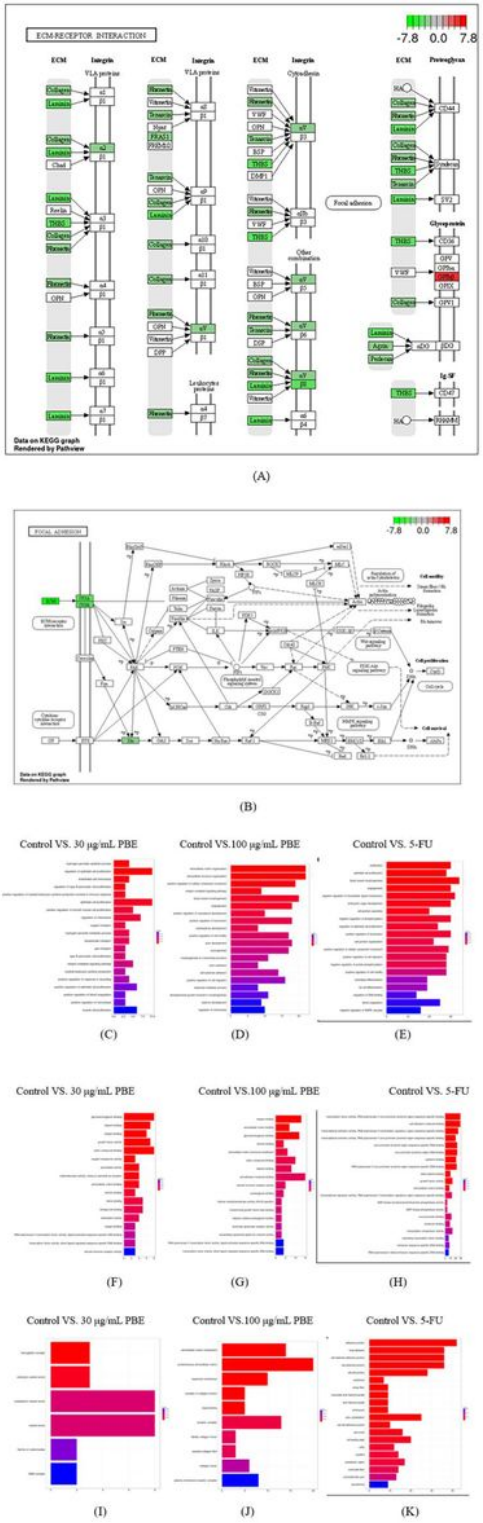

Figure 4

KEGG Pathway and GO Enrichment Analysis. ECM-receptor interactions (A) and FA (B) signaling pathways were downregulated in response to PBE (KEGG) with biological processes (C, D, and E), molecular function (F, G, and H), and cellular components (I, J, and K) being the most affected when evaluated by GO.

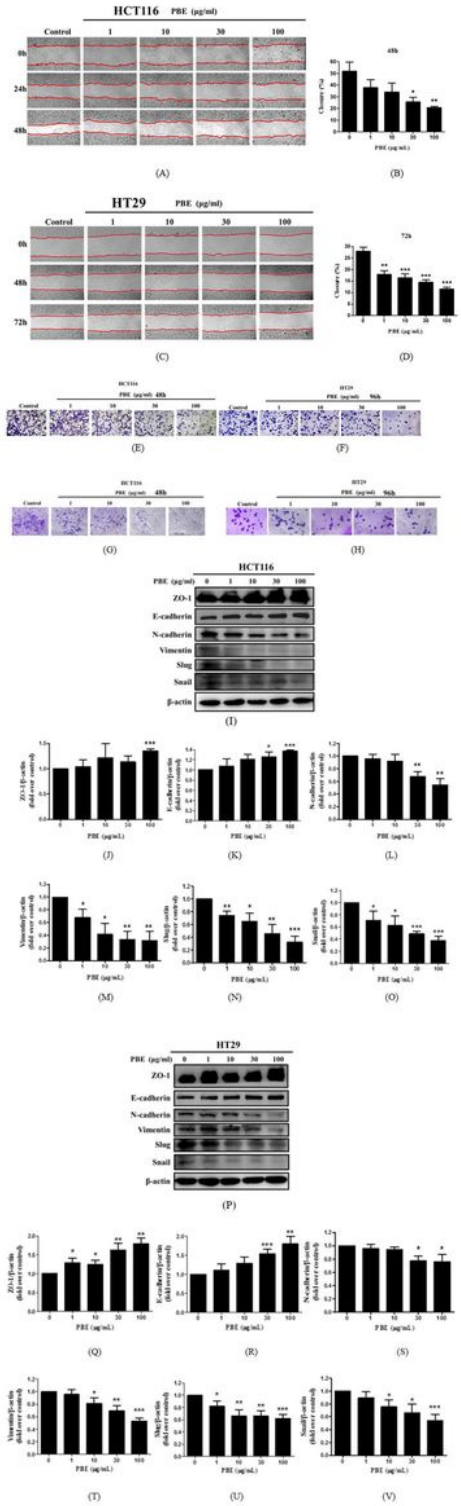

Figure 5

Effect of PBE on cell migration, invasion, and EMT Cell migration was analyzed using both scratch (A-D) and migration assays (E and F) following 48 h or 72 h of treatment with PBE. Cellular invasion assays were completed following 48 h or 96 h of treatment with PBE. (G and H). EMT markers in both HCT116 (I-O) and HT29 (P-V) cells were evaluated by western blot following 72 h of treatment with PBE. Data are

presented as the mean ± SEM from three independent experiments. *p<0.05, **p<0.01, and ***p<0.001 vs vehicle-treated cells.

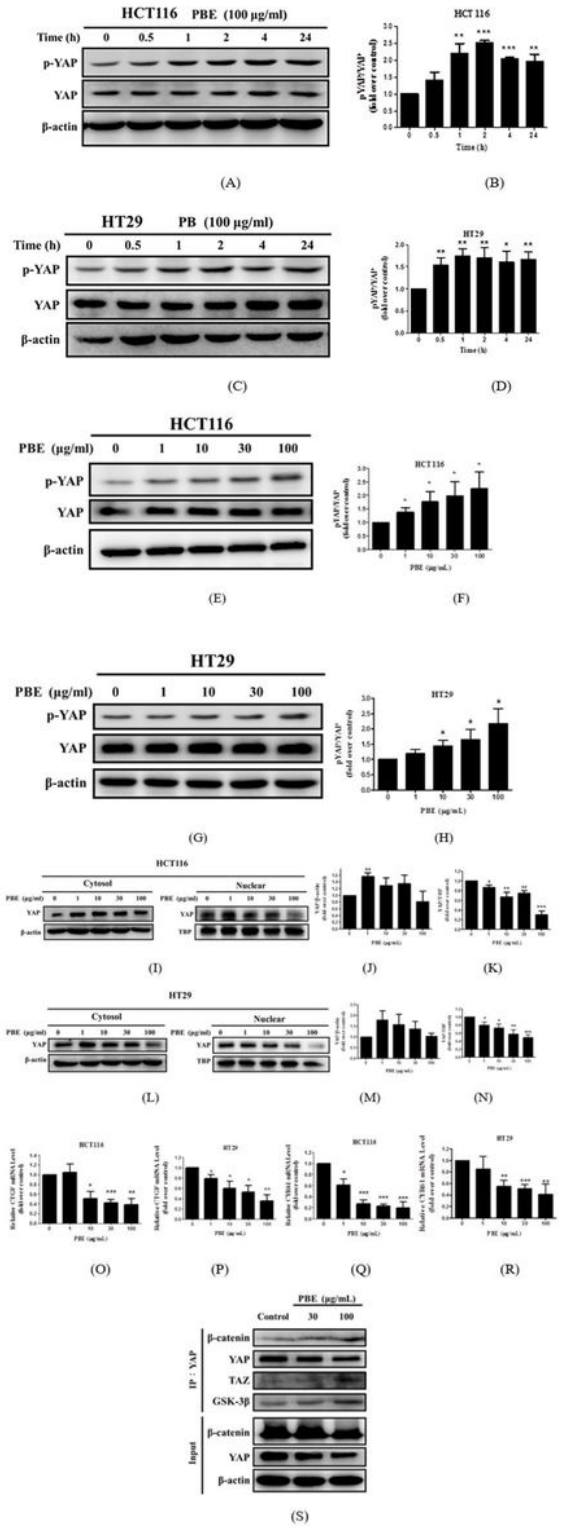

Figure 6

Effect of PBE on the YAP signaling pathway Phosphorylation of YAP following PBE treatment was analyzed using western blotting and evaluated in terms of both time (A-D) and dose dependency (E-H). Nuclear and cytosolic translocation of YAP was also evaluated in both cell lines (I-N). The relative

expression of CTGF and CYR61 was determined using quantitative PCR (O-R) and Co-IP was used to evaluate the interactions between YAP, β-catenin, and GSK-3β (S). Data are presented as the mean ± SEM from three independent experiments. *p<0.05, **p<0.01, and ***p<0.001 vs vehicle-treated cells.

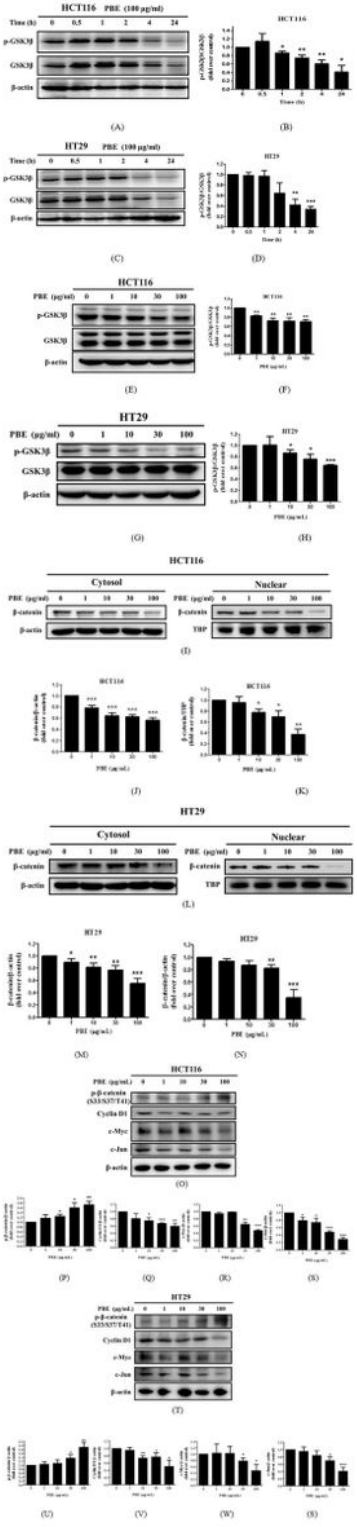

Figure 7

Effect of PBE on the GSK3β/β-catenin signaling pathway Phosphorylation of GSK3β was evaluated in terms of both time (A-D) and dose dependency (E-H) using western blotting. Nuclear and cytosolic

translocation of β-catenin was also evaluated in both cell lines (I-N) and the protein levels of cyclin D1, c-Myc, and c-Jun were analyzed and quantified (O-X). Data are presented as the mean ± SEM from three independent experiments. *p<0.05, **p<0.01, and ***p<0.001 vs vehicle-treated cells.

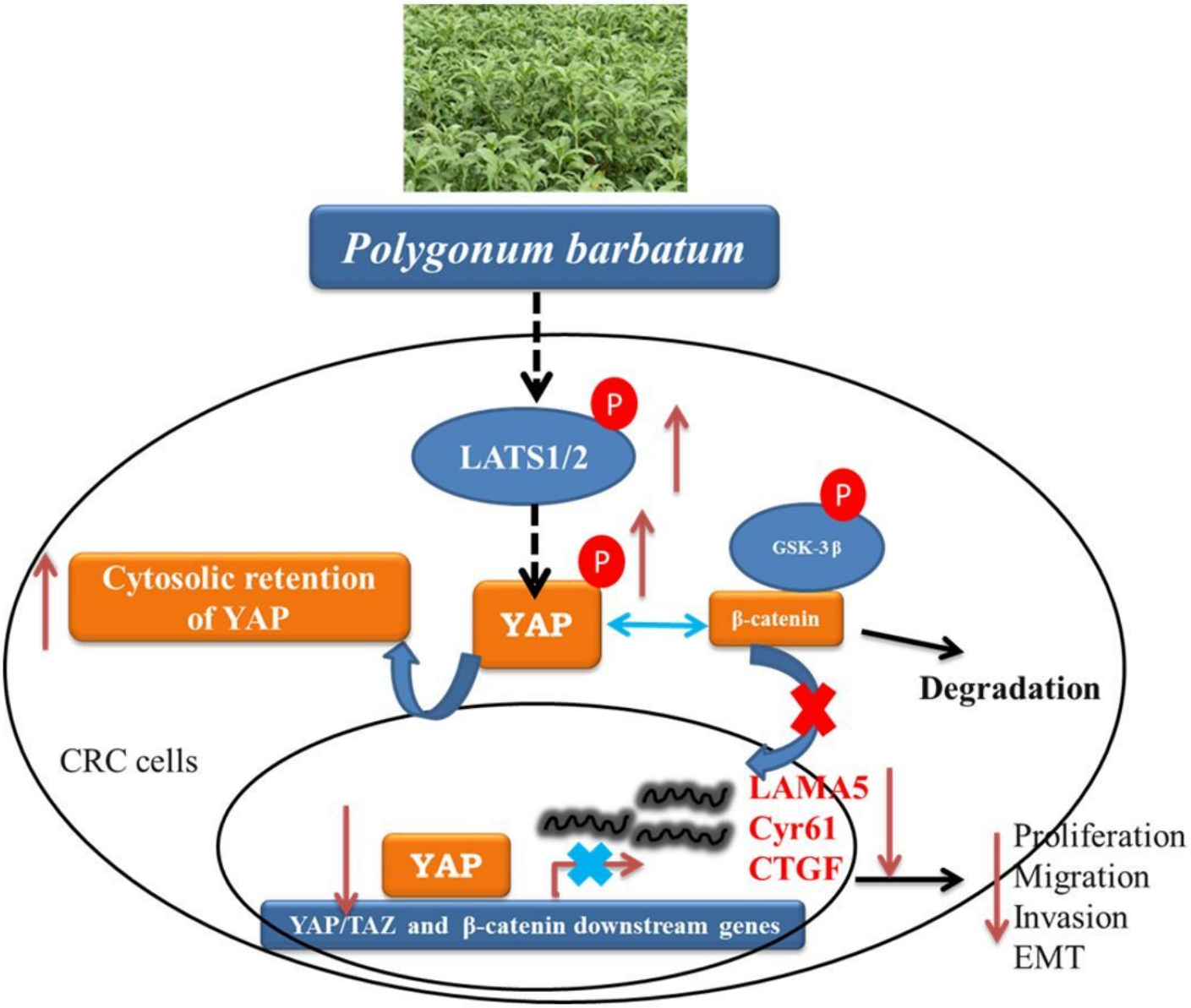

Figure 8

Proposed mechanisms of action for PBE in CRC cells. PBE increases the phosphorylation of YAP and blocks WNT signaling, decreasing cell adhesion and ECM stiffness, resulting in the inhibition of CRC cell invasion and migration.